To determine the composition of these noncondensable reaction products, the reactor containing the products from the OF_2—B_2H_6 reaction was opened to an evacuated bulb through a cold trap held at −195°C. A mass spectral analysis, performed by M. Frech of the Jet Propulsion Laboratory, showed that better than 99% of the material transferred to the bulb was H_2. An infrared spectrum of a sample of the constituents retained in the cold trap is shown in Fig. 5. Identifiable compounds included BF_3, HBF_2, and SiF_4. A peak at 8.7 μ was attributed to B_2F_4, but that identification was uncertain. The BF_3 was definitely the predominant reaction product. If the reaction between OF_2 and B_2H_6 were assumed to be

$$3OF_2 + 3B_2H_6 \rightarrow B_2O_3 + 2B + 2BF_3 + 9H_2,$$

then the calculated final pressure for 40-torr initial pressure would be 73.3 torr, a value very close to the observed 71 torr. The reaction equation assumed that nonvolatile boron and B_2O_3 would have been formed as products of the B_2H_6—OF_2 reaction. The presence of solid products was verified experimentally when 200 mm of F_2 was added to the evacuated reactor and heated to 600°C; the resulting gases were pumped out through a Pyrex trap, indicating the pressure of BF_3 and SiF_4 (the latter having resulted from the reaction of F_2 with the Pyrex). The BF_3 must have come from nonvolatile materials in the reactor by such reactions as

$$B_2O_3 + 3F_2 \rightarrow 2BF_3 + \tfrac{3}{2}O_2$$

and

$$B + \tfrac{3}{2}F_2 \rightarrow BF_3$$

and its existence serves to substantiate the reaction equation noted previously. The composition of the solid materials is likely to be more complex than a mixture of B and B_2O_3, and may well consist of polymeric materials containing B, H, and O. Further studies are required to determine their nature.

Conclusion

At ambient temperatures and low pressures, OF_2 and B_2H_6 react slowly to produce mostly BF_3 and probably H_2 as volatile products. Mixtures of OF_2 and B_2H_6 can coexist at −195°C, but they can also explode while warming to ambient temperature. When these compounds are heated together, nonvolatile boron compounds, along with BF_3, H_2, and smaller amounts of HBF_2 and possibly B_2F_4, are produced. The reaction of an equimolar mixture of OF_2 and B_2H_6 may be tentatively represented as

$$3OF_2 + 3B_2H_6 \rightarrow B_2O_3 + 2B + 2BF_3 + 9H_2$$

References

[1] Dawson, B. E. and Schreib, R. R., Jr., "Investigation of Advanced High Energy Space Storable Propellant System–OF_2/B_2H_6," AIAA Paper 238-63, Los Angeles, Calif., 1963.

[2] "Structural Studies of Inorganic Oxidizers," Annual Summary Report RPL-TDR-64-98, 1964, Contract AF 04(611)-9372, Midwest Research Institute, Kansas City, Mo.

[3] Dawson, B. E., Lum, A. F., and Schreib, R. R., Jr., "Investigation of Advanced High Energy Space Storable Propellant," Rept. 5507F, Contract NASw-449, June 1962, Thiokol Chemical Co., Reaction Motors Div., Denville, N.J.

[4] Stock, A., *Hydrides of Boron and Silicon*, Cornell University Press, Ithaca, N.Y., 1933.

[5] Price, W. C., "The Absorption Spectrum of Diborane," *Journal of Chemical Physics*, Vol. 16, No. 9, Sept. 1948, pp. 894–902.

[6] Toy, M. S., Cannon, W. A., and English, W. D., *Solution and Conductivity Studies in Fluorine-Containing Liquid Oxidizers*, DA-31-124-ARO(D)-115, QPR-5, 1964, Astropower Lab., Douglas Aircraft Co., Newport Beach, Calif.

[7] Simons, J. H., *Fluorine Chemistry, Vol. II*, Academic Press, New York, 1954, p. 498.

[8] Coyle, T. D., Ritter, J. J., and Farrar, T. C., "Preparation and Properties of Difluorobane," *Proceedings of the Chemical Society*, Jan. 1964, p. 25.

[9] Finch, A., Hyams, I., and Steele, D., "The Vibrational Spectra of Diboron Compounds. I. Infrared Spectra of Diboron Tetrafluoride," *Spectrochimica Acta*, Vol. 21, No. 8, Aug. 1965, pp. 1423–1431.

[10] Fisher, H. D., Kiehl, J., and Cane, A., *Infrared Spectra and Thermodynamic Properties of Trifluoroboroxine* (FBO_3), Rept. R-HTC-61-90, Contract AF 33(616)-6781, 1961, Hughes Tool Co., Culver City, Calif.

[11] Coggeshall, N. D. and Saier, E. L., "Pressure Broadening in the Infrared and Optical Collision Diameters," *Journal of Chemical Physics*, Vol. 15, No. 1, 1947, pp. 65–71.

[12] Goldstein, M. S., "The Oxidation of Diborane," PhD thesis, Feb. 1960, Rensselaer Polytechnic Institute, Chemistry Dept., Troy, N.Y.

Nonsteady Flow past Duct Junctures

A. W. Zimmerman,* J. B. Peterson,† and H. J. Carpenter‡

TRW Systems Group, Redondo Beach, Calif.

Nomenclature

D	=	hydraulic diameter
$\bar{f}$	=	defined by Eq. (3)
h	=	enthalpy per unit mass
$L_{MAX}(M)$	=	length of duct for steady adiabatic flow to be accelerated by friction from M to $M = 1$
M	=	Mach number
P	=	pressure; $P_{ij} = P_i/P_j$
R	=	radius or gas constant
T	=	temperature
t	=	time
u	=	velocity
x	=	distance
γ	=	ratio of specific heats
Δq	=	nondimensional momentum loss defined by Eq. (2)
ρ	=	density
τ_w	=	shear stress at wall

Subscripts

t	=	stagnation property
1,2, . . .	=	flow regions (indicated on figures)

Superscript

*	=	sonic point property

1. Introduction

A VENTILATION system for an underground bomb shelter must be designed to prevent the passage of a bomb-produced blast wave into the installation. A blast valve triggered in advance of shock arrival may be used. For analyses of blast loads, a method for treating the flow in the neighborhood of duct junctures is needed. In general, this flow will be three-dimensional and viscous, and complex wave interactions will occur. However, a duct juncture is typically a small part of a duct system, and the time required to establish quasi-steady flow in the juncture is much shorter than for the ventilation system as a whole. We will assume

Received September 19, 1969; revision received November 6, 1969. Research sponsored by U.S. Air Force Contracts AF-04(694)-907 and AF-04(694)-908.

* Member of the Technical Staff, Aerosciences Laboratory. Member AIAA.

† Section Head, Aerosciences Laboratory. Member AIAA.

‡ Department Manager, Vulnerability and Hardness Laboratory. Member AIAA.

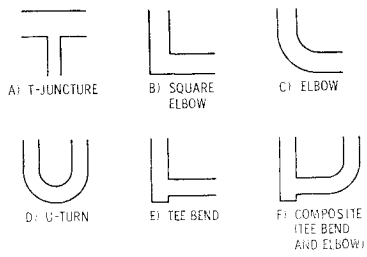

Fig. 1 Duct junctures tested.

that, for the blast-wave problem, the junctures may be characterized by over-all steady-flow losses, which may be used to determine boundary conditions for one-dimensional, unsteady analyses of the flowfields upstream and/or downstream of the juncture.

The duct junctures considered (see Fig. 1) fall into two principle types: the T-juncture and the constant-area bend. For a side-on surface entrance (Fig. 2; equivalent to a T-juncture with an infinite area ratio) or T-juncture, the ratio of stagnation pressure of the entrance flow P_t to the static pressure of the surface flow P_2 is determined as a function of the flow Mach numbers outside and within the entrance. For a constant-area bend, overall momentum loss is obtained as a function of bend geometry. Finally, the application of these results to analysis of the flow upstream or downstream of a juncture is discussed.

2. Side-On Entrance

2.1 *Analytical approach*

The problem is to determine the properties at a boundary point (C in Fig. 2) for the flow in the side duct when properties at points A and B (Fig. 2) are known. Heat transfer from the gas may be neglected, hence $T_{t5} = T_{t2}$. A second condition is a compatibility relation with the flow downstream of the entrance, e.g., the wave equation along the characteristic from B to C. Specification of P_{t5} completes the problem. The quantity P_{t5}/P_2 was determined from measurements of (P_2/P_1) and (P_4/P_1) in a T-juncture with a large area ratio (ratio of main duct area to side duct area). If there were no losses, P_{t5} would be equal to P_{t2}, but one observes that $P_{t5} < P_2$ for $M_2 \gtrsim 0.2$.

If $M_2 > 1$ and the flow is steady in region 5 (Fig. 2), then knowledge of P_2 and $P_5 = P_4$ uniquely determines P_{t5}/P_2. If $M_5 > 1$, steady acceleration implies the existence of an effective throat at the entrance. An alternate assumption is that the acceleration in region 5 is steady to the sonic line and nonsteady thereafter. The strength of the rarefaction is determined since

$$h_{t2} = h^* + u^{*2}/2 = h^* + \gamma RT^*/2 \qquad (1)$$

If $M_2 < 1$, a rarefaction propagates upstream from the T-juncture and a third measurement (the pressure downstream of the T-juncture in the main duct) is required. This rarefaction can be neglected in a large area ratio T-juncture.

2.2 *Experimental apparatus, results, and discussion*

The experimental work was done by the Illinois Institute of Technology Research Institute using a T-juncture with an area ratio of 7.3. Comparison of the results (Fig. 3a) with

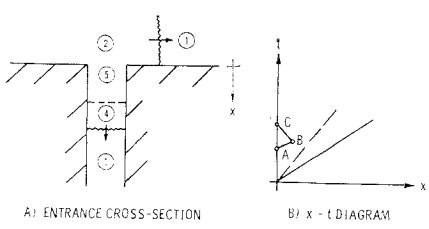

Fig. 2 Surface entrance wave motion.

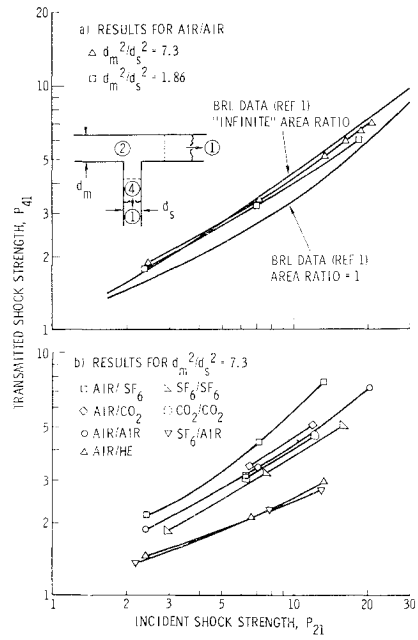

Fig. 3 Transmitted vs incident shock strength for T-junctures with various area ratios and for different combinations of gases (gas initially in main duct/gas initially in side duct). Each point of these graphs represents an average for a group of tests, usually three.

experiments done with a T-juncture having an area ratio of 1.86 and with surface entrance experiments done by Ballistic Research Laboratories[1] justifies the choice of area ratio; an increase beyond 7.3 would not significantly increase the transmitted shock strengths obtained.

The T-juncture was provided with a thin diaphragm retainer at the juncture between the main and side ducts, so that the two ducts could be filled with dissimiliar gases prior to testing. Then the molecular weight of the gas in the side duct was varied to obtain P_{t5}/P_2 as a function of M_5. A square§ wave was driven into the model by a 2-in.-i.d. shock tube. Cold helium was used as the driver, and combinations of He, air, CO_2, and SF_6 were used as driven gases. The driven chamber(s) was filled to 1 atm in every case. Eight piezoelectric gauges at ~1 ft spacings were used in the models to provide time-of-arrival data and pressure-time histories. Shock pressure ratios were calculated from the time-of-arrival data. The experiments are discussed in greater detail in Ref. 2.

The data from a typical set of four tests are presented in Fig. 4. Figure 3b presents the T-juncture data in the form of incident (P_{21}) vs transmitted (P_{41}) shock pressure ratios, which were obtained by extrapolating, to the juncture, the pressures obtained by the upstream and downstream gauges.

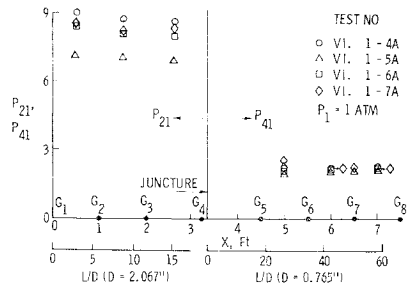

Fig. 4 Typical T-juncture test data. Data obtained in a T-juncture (area ratio = 7.3) with SF_6 initially in main duct and air initially in side duct.

§ The test duration was long enough so that the interface or reflected rarefaction did not affect the test results.

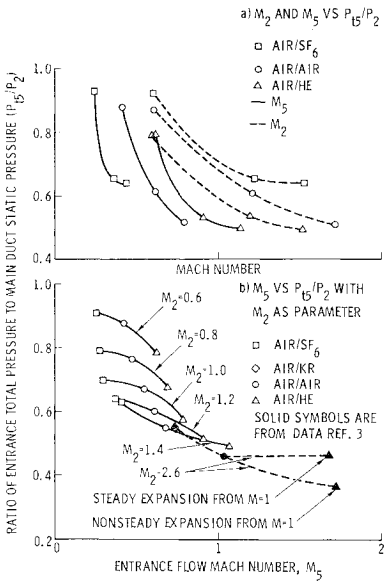

Fig. 5 Ratio of entrance total pressure to main duct static pressure (T-juncture area ratio = 7.3) vs Mach numbers of flow inside and outside entrance.

From these data, M_2, M_5, and P_{t5}/P_2 were calculated assuming air and SF_6 to be thermally perfect but not calorically perfect. Helium was assumed to be perfect. The information in Fig. 5a is cross plotted in Fig. 5b to give P_{t5} vs M_5 for specific surface Mach numbers. The curves are all expected to go through the point $P_{t5}/P_2 = 1$, $M_5 = 0$, although appearances are to the contrary.

Results from more recent tests at substantially higher pressures by the Stanford Research Institute[3] are also shown in Fig. 5b. A Mollier chart for equilibrium real air was used in reducing the data. It is significant that the dependence of P_{t5}/P_2 on M_2 is very weak when $M_2 > 1.4$. The air/He data were reduced in two ways: 1) assuming a nonsteady expansion downstream of the sonic line in the side duct, and 2) assuming a steady expansion to M_5. Investigation of the flow structure in the neighborhood of the tee is necessary to determine which (if either) of the two assumptions is most appropriate.

3. Constant-Area Bends

3.1 *Analytical approach*

The shock strength transmitted by a bend is less than the incident shock strength, and one observes a reflected shock. It is postulated that a bend may be considered a discontinuity across which flow properties are joined by a Fanno line. A x-t diagram for a shock wave interaction with a Fanno region of infinitesimal extent is shown in Fig. 6. The flow is accelerated by friction in the bend, and if P_{21} is high enough (>6 in air) the flow leaves the Fanno region at sonic velocity and further acceleration is nonsteady. In this case (of greatest practical interest), the flow is choked by the bend and the upstream flow is decoupled from the downstream flow. Within the Fanno region, the flow accelerates steadily from M_3 (which is dependent only on the normalized mo-

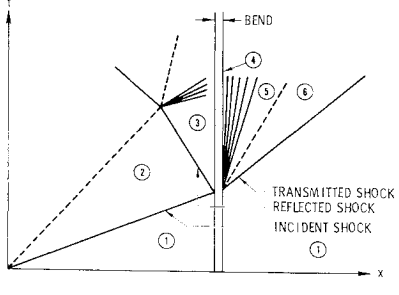

Fig. 6 Wave diagram for shock interaction with a bend.

Table 1 Bend momentum loss results (choked flow only)

Type	Number of tests	P_{21}	Δq
90° Elbow (R/D = 1.5)	5	6.7	0.7
	5	14	0.7
	3	7.3	0.5
	3	14.5	1.0
90° Square elbow	3	6.0	1.0
	3	12.3	1.7
180° Turn (R/D = 1.5)	4	6.6	0.8
	3	16.5	0.9
	4	6.6	0.2
Tee bend	8	6.7	2.0
	5	16	1.8
	3	7.0	1.8
Composite	3	7.0	2.6
	3	14	3.0

mentum loss (Δq) when the flow is choked) to $M_4 = 1$. Hence Δq should be independent of P_{21} in the choked regime. From Shapiro[4]

$$\Delta q = (4/D)[(\bar{f}L_{\mathrm{MAX}})_{M_3} - (\bar{f}L_{\mathrm{MAX}})_{M_4}] \tag{2}$$

where

$$\bar{f} = \frac{1}{L_{\mathrm{MAX}}} \int_0^{L_{\max}} \left(\frac{2\tau_w}{\rho u^2}\right) dx \tag{3}$$

Momentum losses were obtained experimentally for various constant-area bends by measuring P_{21} and P_{41} and comparing the measurements with P_{41} calculated as a function of Δq and P_{21}. Perfect-gas relations were used for the calculations. Straight-tube viscous decay was eliminated by comparing P_{41} vs distance downstream of the bend with comparable straight-tube results.

3.2 *Experimental apparatus, results, and discussion*

The shock tube previously described was also used for the bend experiments. The placement of the gages in one of the models (the Tee Bend) is indicated in Fig. 7. The curve labelled "st. tube decay curve" was obtained in a straight tube with P_{21} (1), Reynold's number, and the distance from the diaphragm to the first gage held constant. The displacement of the bend data from the st. tube curve represents the bend momentum loss. For cases where this displacement had not reached a clear asymptotic value, the difference at the last or next to last measuring station was used to calculate Δq.

The results are presented in Table 1. Within the accuracy obtained, the expectation that Δq is independent of P_{21} appears to be confirmed. Also, the magnitude of the loss for the mitre bend agrees approximately with results obtained independently. From steady flow tests with a mitre bend of circular cross section, $\Delta q = 1.0$ is reported[5] for the choked condition, and an unpublished two-dimensional shock propa-

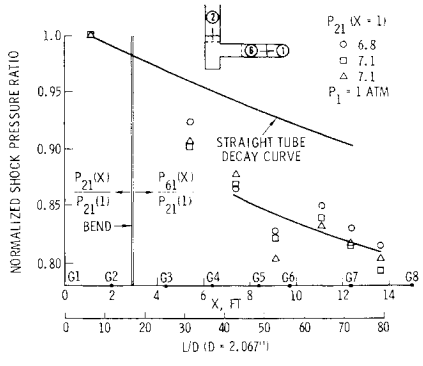

Fig. 7 Typical constant-area bend test results.

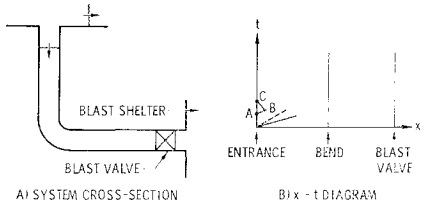

Fig. 8 Simple blast shelter ventilation system.

gation calculation ($P_{21} = 18$) by the Los Alamos Scientific Laboratory yielded $\Delta q = 1.2$.

All the results are based on measurements of P_{41}. The reflected shock pressure ratio P_{32} (Fig. 6) is more sensitive to Δq, however, the reflected shock intersects the interface within inches of the bend and it interacts with the boundary layer.

Finally, the radius elbow results are not satisfactory. First the expected reduction in P_{61} is comparable with the experimental accuracy. Further, the data suggest that the transmitted shock strength is recovering (approaching the st.-tube decay curve) at the last gage. This observation is consistent with results[5] from steady flow tests. Ref. 5 gives for the choked condition: 90° elbow, $R/D = 1.0$ and 2.0, $\Delta q = 0.19$ and 0.12; 180° elbow, $R/D = 1.0$ and 2.0, $\Delta q = 0.29$ and 0.14. Evidently, the losses obtained for the low-resistance bends are much too high. The high-resistance bend results, on the other hand, are probably correct within the accuracy obtained.

4. Application of Results

To illustrate the application of the data, let us consider the simple ventilation system in Fig. 8. To simplify the problem, individual bend losses have been lumped together at one location. The blast valve is assumed to close before shock arrival, and the load on the valve is desired. A description of the flow over the entrance is assumed known. An adequate description (beyond the range where radiation coupling with the flow is important) is that given by Brode[6] for a TNT burst.

Sufficient boundary conditions at the entrance are $h_t(t)$ and $P_t(t)$. The blast description gives $h_t(t)$ (neglecting heat transfer to the entrance), $M_2(t)$, and $P_2(t)$. Then P_t is chosen, at each point in the calculation, to satisfy simultaneously the curves in Fig. 5b and the wave equation along the characteristic from B to C (Fig. 8). If the entrance is choked, M_5 is taken to be unity, although the data (Fig. 5b) appear to indicate a further loss as the flow goes supersonic.

The flowfield is divided at the bend into two one-dimensional segments. The upstream boundary condition is a constant Mach number if the flow is choked by the bend; this M is a function of Δq and γ. If $\Delta q = 1$, $\gamma = 1.4$, for example, $M \simeq 0.51$ from Table B.4 of Ref. 4. If the flow is not choked, the two flowfields are not decoupled, and ΔM across the bend is chosen at each step so that Δq remains constant. The boundary condition at the valve is that $M = 0$.

References

[1] "Information Summary of Blast Patterns in Tunnels and Chambers (Second Edition)," Rept. 1390, March 1962, Ballistic Research Labs., Aberdeen Proving Ground, Md.

[2] Zimmerman, A. W., "Flow Through Duct Junctures of a Hardened Ventilation System Due to a Nuclear Blast," 11466-6055-R00-00, Dec. 1968, TRW Systems, Redondo Beach, Calif.

[3] Bredfeldt, H. R., Berke, J. G., and Goettelman, R. C., "Measurements of Shock Wave Attenuation in Various Duct Components—Phase 1," Final Report, Proj. PGU 6867, Aug. 1968, Stanford Research Institute, Menlo Park, Calif.

[4] Shapiro, A. H., *The Dynamics and Thermodynamics of Compressible Fluid Flow*, Vol. 1, Ronald Press, New York, 1953, Chap. 6.

[5] "Engineering Fundamentals," *Aero Space Applied Thermodynamics Manual*, revised ed., Society of Automotive Engineers, Jan. 1962, pp. B-97–B-111.

[6] Brode, H. L., "Blast Wave from a Spherical Charge," *The Physics of Fluids*, Vol. 2, No. 2, Feb. 1959, pp. 217–229.

Secondary Peripheral Injection Effects on Axisymmetric Flow

T. F. Beasley*
The Boeing Company, Huntsville, Ala.
AND
D. M. Adams†
DEK Inc., Huntsville, Ala.
AND
R. I. Vachon‡
Auburn University, Auburn, Ala.

Nomenclature

A	=	cross-sectional flow area, ft²
A_{stp}	=	projected area of step at secondary slot exit, $A_1 - A_2$, ft²
a	=	sonic velocity, $(\gamma gRT)^{1/2}$, fps
c_p	=	constant pressure specific heat, $\gamma R/(\gamma - 1)$, Btu/lbm-°R
c_v	=	constant volume specific heat, Btu/lbm-°R
D	=	inside tube diameter, ft
g	=	acceleration of gravity, ft/sec²
h	=	height of step at secondary slot exit, ft
K_1,K_2,K_3	=	coefficients defined by Eqs. (3) and (4)
M	=	Mach number, V/a
$\dot{m}$	=	mass flowrate, lbm/sec
P,P_o	=	static and stagnation pressures, psia
R	=	gas constant, ft-lbf/lbm-°R
T	=	static temperature, °R
V,V_{CL}	=	mean and center-line velocities, fps
w	=	slot width normal to secondary flow, ft
x	=	axial distance from downstream edge of secondary slot, ft
α,β	=	coefficients defined by Eqs. (8)
θ	=	injection angle, °
ρ	=	density, lbm/ft³
γ	=	specific heat ratio (c_p/c_v)

Subscripts

1,2	=	primary sections upstream and downstream of the injection slot, respectively
s	=	secondary slot section at point just before entering the primary flow
x	=	property corresponding to axial position x
min, max	=	minimum and maximum property values in the flow interaction region

Introduction

INTEREST in flow phenomena associated with secondary injection stems from work in the areas of thrust magnitude control[1] and the design of slotted-tube solid propellant motors.[2,3] Other studies[4–6] are concerned with thrust vector control and have centered on two-dimensional and axisymmetric nozzles with injection from one side of the nozzle.

This Note describes an analytical and experimental investigation of the effects of secondary peripheral air injection

Received September 29, 1969; revision received November 4, 1969.

* Research Engineer, Structures and Propulsion Section.
† Consultant, Research Engineer. Member AIAA.
‡ Alumni Professor of Mechanical Engineering. Member AIAA.